

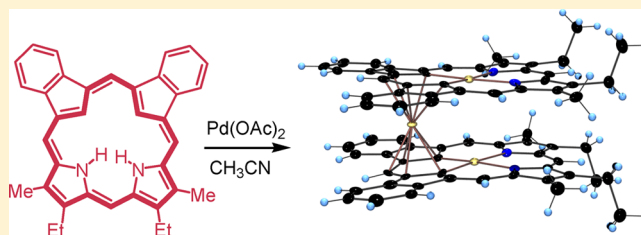
Synthesis of an *adj*-Dicarbaporphyrin and the Formation of an Unprecedented Tripalladium Sandwich Complex

Deyaa I. AbuSalim, Gregory M. Ferrence, and Timothy D. Lash*

Department of Chemistry, Illinois State University, Normal, Illinois 61790-4160, United States

S Supporting Information

ABSTRACT: An *adj*-dicarbaporphyrin was prepared by carrying out a base-catalyzed MacDonald reaction between bis(3-indenyl)methane and a dipyrromethane dialdehyde. The porphyrinoid system exhibited highly diatropic characteristics, and the proton NMR spectrum gave resonances at -5.74 and -6.24 ppm for the internal NH and CH protons, respectively. The UV-vis spectrum was also porphyrin-like, giving a Soret band at 455 nm and a series of Q bands at longer wavelengths. Addition of trifluoroacetic acid gave a C-protonated monocation, and at higher acid concentrations a dicationic species was observed. Addition of 1,8-diazabicyclo[5.4.0]undec-7-ene (DBU) afforded a monodeprotonated porphyrinoid anion. All of these species retained highly diatropic characteristics. Density functional theory calculations showed that a nonplanar tautomer with four internal hydrogens was favored, in agreement with the spectroscopic data. Nucleus-independent chemical shift calculations also confirmed the aromatic characteristics of the free-base, cationic, and anionic structures. The dicarbaporphyrin reacted with palladium(II) acetate in refluxing acetonitrile to give an unusual tripalladium sandwich complex consisting of two dianionic palladium(II) dicarbaporphyrin units surrounding a palladium(IV) cation with unique η^5 interactions involving *meso*-carbon atoms.



INTRODUCTION

Carbaporphyrins (e.g., **1**) are porphyrin analogues in which one of the pyrrolic nitrogen atoms has been replaced by carbon.^{1–3} Although carbaporphyrins^{4,5} and related carbaporphyrinoid systems have been well-studied,^{1,2} little work has been carried out on dicarbaporphyrins.⁶ Carbaporphyrins have been shown to be highly diatropic species, and the proton NMR spectra for structures like **1** give *meso*-proton resonances downfield at values close to +10 ppm, while the internal NH and CH protons typically show up near -4 and -7 ppm, respectively.^{4,5} Carbaporphyrins undergo mono- and diprotonation to give the related monocations 1H^+ and dications 1H_2^{2+} (Scheme 1), the formation of the latter species involving a C-protonation.^{4,5} Carbaporphyrins **1** act as trianionic ligands and form stable silver(III) and gold(III) organometallic derivatives **2**.⁷ N-Alkylated carbaporphyrins afford palladium(II) complexes **3**,⁸ while oxacarboraphyrins generate Ni(II), Pd(II), and Pt(II) derivatives.⁹ In addition, carbaporphyrins **1** undergo regioselective oxidation with excess ferric chloride in the presence of alcohol solvents to afford carbaporphyrin ketals **4**.¹⁰ These unusual structures retain fully aromatic characteristics but exhibit highly modified UV-vis spectra that produce strong absorptions in the far red. The ketal derivatives have also been shown to be effective agents in the treatment of leishmaniasis.¹¹

An example of a dicarbaporphyrin with two opposite indene subunits, **5**, was reported 15 years ago^{6,12} but has been little-studied because of its poor stability. Nevertheless, this system exhibits aromatic properties, and the proton NMR spectrum of **5** in CDCl_3 gave upfield resonances for the internal NH and

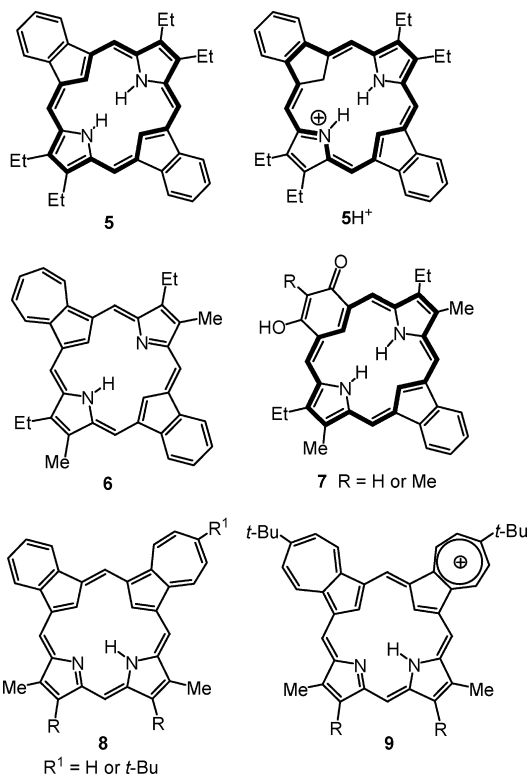
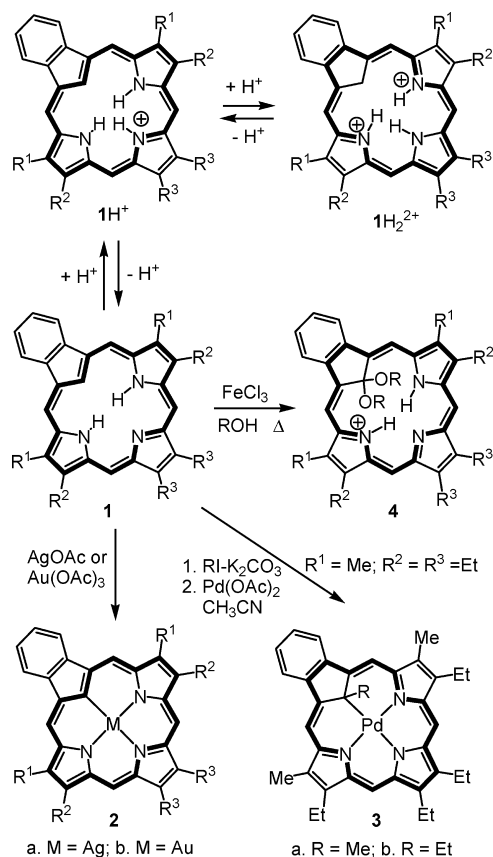
CH units at -4.8 and -5.7 ppm, respectively. Addition of trace amounts of trifluoroacetic acid (TFA) to solutions of **5** resulted in the formation of the C-protonated cation 5H^+ .⁶ *opp*-Dicarbaporphyrinoid **6** with azulene and indene subunits was reported, but this system also was somewhat unstable.¹³ Resorcinol-containing dicarbaporphyrinoids **7** have also been obtained but have been little-studied because of their poor solubility in most organic solvents.¹⁴ Superior results were obtained with carbaporphyrinoids possessing two adjacent carbocyclic rings. 22-Carbaazuliporphyrin **8**, an isomer of **6**, proved to be quite stable,¹⁵ although attempts to metalate this structure have been unsuccessful. In addition, an *adj*-diazuliporphyrin has been reported, and this system was found to be quite stable in the protonated form 9H^+ or as the related dication.¹⁶ However, syntheses of *adj*-dicarbaporphyrins with two cyclopentadiene or indene rings and two pyrrole rings have not been reported previously.

We recently demonstrated that bis(3-indenyl)methane (**10**) reacts with furfural in the presence of potassium hydroxide to give the bilin analogue **11** (Scheme 2).¹⁷ Cyclization of **11** with aromatic aldehydes in the presence of boron trifluoride etherate followed by brief treatment with DDQ then gives dioxadibaporphyrins **12**.¹⁷ As expected, these porphyrinoids exhibit strongly aromatic characteristics. In the presence of excess TFA, the C-protonated cation 12H^+ is generated (Scheme 2).¹⁷

Received: March 20, 2014

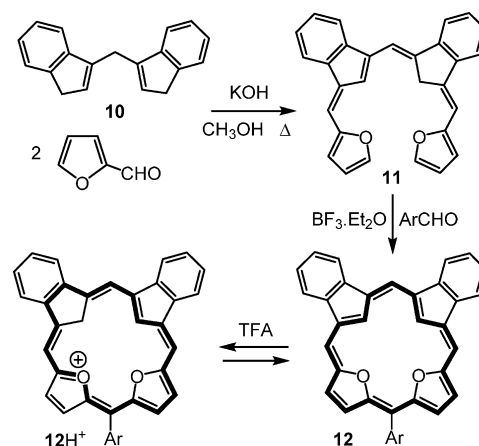
Published: April 16, 2014

Scheme 1

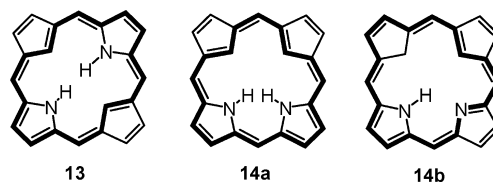


Dicarbaporphyrinoids with adjacent carbocyclic rings have been shown to be far more robust than the corresponding *opp*-dicarbaporphyrinoids.^{15,16} However, density functional theory (DFT) calculations indicated that *opp*-dicarbaporphyrin 13 is

Scheme 2



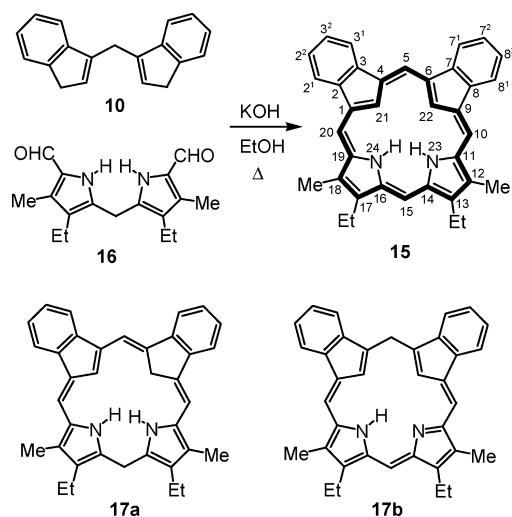
more stable than *adj*-dicarbaporphyrin 14.¹⁸ Furthermore, these calculations predicted that the tautomer 14b with an internal CH_2 is favored over the more conventional structure 14a.¹⁸ Nevertheless, *adj*-dibenzodibenzoporphyrin 15 (Scheme 3) was considered to be an important target to further our understanding of these systems. In this paper, we report the first synthesis of an *adj*-dicarbaporphyrin using a base-catalyzed version of the MacDonald reaction.¹⁹ The protonation and deprotonation behavior of this system was investigated, and the aromatic properties were assessed using spectroscopic and computational techniques. In addition, a very unusual palladium complex of this system is described.



RESULTS AND DISCUSSION

It was anticipated that an *adj*-dicarbaporphyrin 15 could be prepared by a “2 + 2” condensation between diindenylmethane 10 and dipyrromethane dialdehyde 16 (Scheme 3). This

Scheme 3



represents a previously unexplored base-catalyzed version of the MacDonald reaction. Diindenylmethane **10** has previously been shown to react with aromatic aldehydes and potassium hydroxide in refluxing methanol to give bilin analogues such as **11** (Scheme 2).¹⁷ However, pyrrole aldehydes have greatly reduced reactivity because of their associated vinylogous amide characteristics, and the formation of fulvene-type derivatives from these intermediates was far from assured. Nevertheless, when **10** was reacted with **16** and potassium hydroxide in refluxing ethanol for 4 days, the targeted porphyrinoid **15** was isolated in 21% yield. In principle, a dihydroporphyrinoid such as **17a** or **17b** should be generated initially, but these intermediates appear to undergo spontaneous oxidation to the fully aromatic dicarbaporphyrin upon exposure to air. The new porphyrinoid was reasonably stable in solution and was isolated as a dark-blue powder after recrystallization from chloroform/hexanes. The UV–vis spectrum of **15** in chloroform was porphyrin-like, showing a strong Soret band at 455 nm and Q bands at 542, 579, and 657 nm (Figure 1). Addition

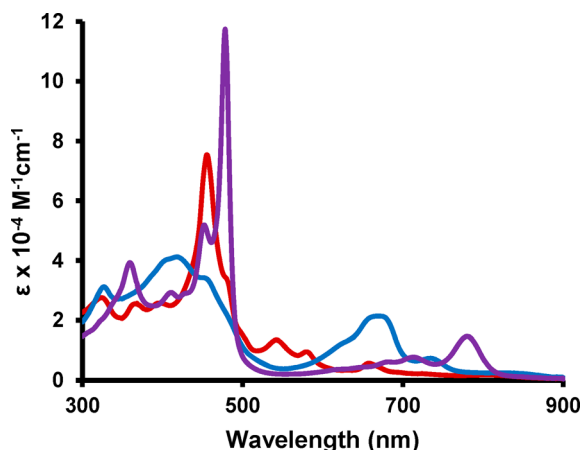


Figure 1. UV–vis spectra of dicarbaporphyrin **15** in chloroform (free base, red line), 5% TFA/ CHCl_3 (monocation 15H^+ , blue line), and HCl/TFA (dication 15H_2^{2+} , purple line).

of TFA resulted in the formation of a new species that was assigned as cation 15H^+ (Scheme 4), and it showed a far weaker and broadened absorption at 418 nm and broad peaks at 670 and 734 nm (Figure 1). As the concentration of acid was increased, a third species was formed that corresponded to the dication 15H_2^{2+} (Scheme 4). In HCl/TFA, this species showed an intensified Soret band at 478 nm and bathochromically shifted Q bands at 713 and 780 nm (Figure 1).

Significant changes to the spectra were also noted upon addition of base (Figure 2). Addition of 1,8-diazabicyclo[5.4.0]-undec-7-ene (DBU) to solutions of **15** in chloroform led to the formation of a new species that exhibited intensified split Soret bands. In 10% DBU/ CHCl_3 , these bands appeared at 465 and 477 nm, together with two Q absorptions at 578 and 620 nm (Figure 2). These results were attributed to the formation of the monodeprotonated species $[15\text{-H}]^-$ (Scheme 5). Further changes were not observed when the concentration of DBU was raised to 90%, indicating that DBU is not sufficiently basic to form the corresponding dianion $[15\text{-2H}]^{2-}$ (Scheme 5). Solutions of anion $[15\text{-H}]^-$ proved to be rather unstable, and the intensities of the absorptions dramatically decreased over a period of 10 min.

Scheme 4

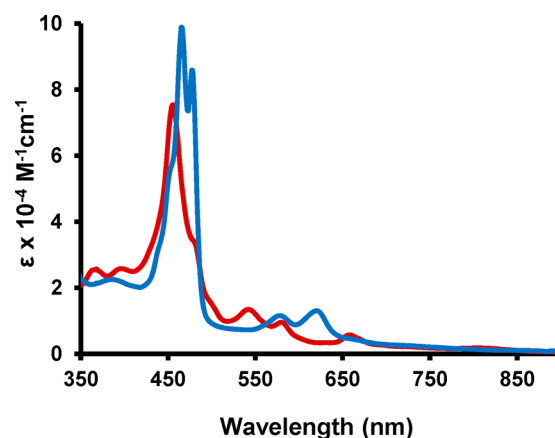
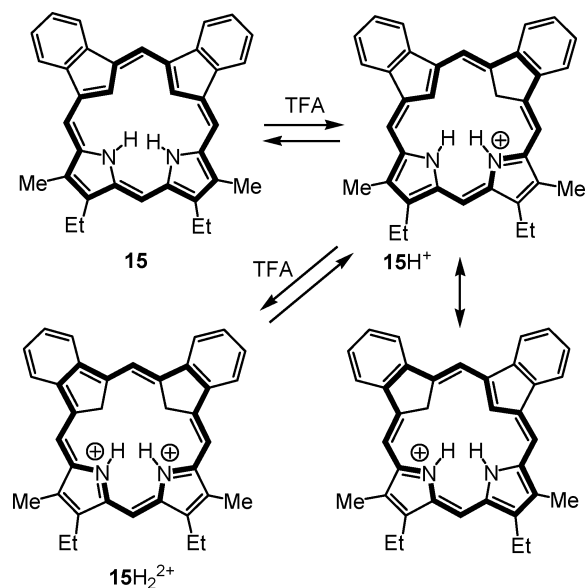
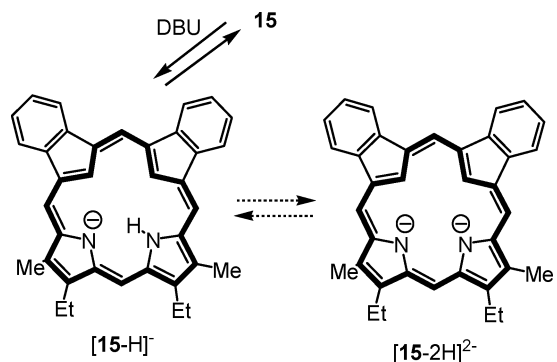


Figure 2. UV–vis spectra of dicarbaporphyrin **15** in chloroform (free base, red line) and 10% DBU/ CHCl_3 (anion $[15\text{-H}]^-$, blue line).

Scheme 5



The proton NMR spectrum of **15** in CDCl_3 showed that this system is highly diatropic (Figure 3) and unequivocally demonstrated that the depicted tautomer is favored over a species related to **14b** possessing an internal methylene unit. The external *meso*-protons were observed as three singlets at 8.91 ppm (1H), 9.09 ppm (2H), and 9.48 ppm (1H), while the interior NH and CH resonances appeared upfield at -5.74 and

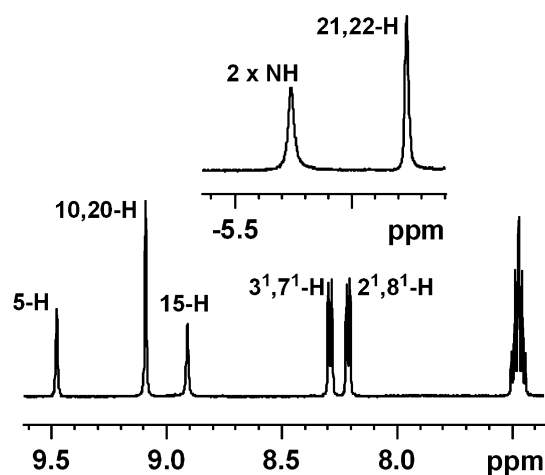


Figure 3. Partial 500 MHz proton NMR spectra of dicarbaporphyrin **15** in CDCl_3 , showing the upfield and downfield regions.

−6.24 ppm, respectively. The carbon-13 NMR spectrum of **15** confirmed the presence of a plane of symmetry and gave resonances for the *meso*-carbons at 87.1, 98.7, and 109.2 ppm, while the internal CH was located at 115.9 ppm. Addition of TFA gave monocation 15H^+ , and this species also exhibited a strong diamagnetic ring current. The interior CH_2 and CH protons gave singlets at −3.61 ppm (2H) and −2.04 ppm (1H), respectively, while the NH units gave broad singlets at −0.40 and −0.02 ppm. The *meso*-protons were all significantly deshielded, giving rise to four 1H singlets at 9.27, 9.54, 9.76, and 9.92 ppm. Methyl groups attached to porphyrins are generally deshielded to values of approximately 3.6 ppm because of the proximity of the aromatic ring current, and these resonances can also be used as a measure of the diatropic character of these structures. In the free base, the methyl groups gave a 6H singlet at 3.24 ppm, while in the asymmetrical monocation 15H^+ , the methyl groups appeared as two 3H resonances at 3.21 and 3.28 ppm. Taken together, these data show that the diatropic characters of **15** and 15H^+ appear to be similar, but both species show reduced shifts relative to porphyrins and carbaporphyrins such as **1**. The proton NMR spectrum of the dication 15H_2^{2+} was obtained in TFA containing several drops of concentrated hydrochloric acid. This species showed the internal methylene units at −4.09 ppm

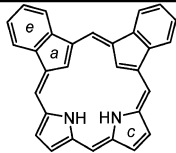
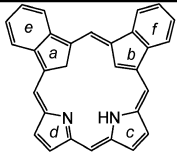
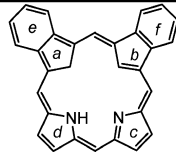
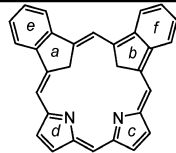
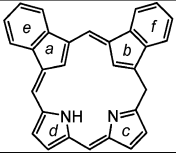
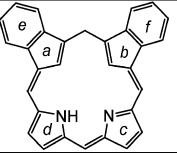
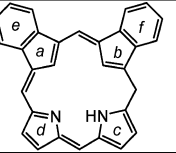
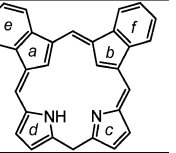
and the NH resonances at −0.49 ppm. The *meso*-protons were shifted further downfield to give singlets at 10.49 ppm (1H), 11.06 ppm (2H), and 12.08 ppm (1H), while the methyl groups gave a 6H singlet at 3.52 ppm. These data indicate that the diatropicity of the dication is enhanced relative to **15** or 15H^+ . The carbon-13 NMR spectrum of 15H_2^{2+} showed that the structure had regained a plane of symmetry. The *meso*-protons were identified at 110.0 ppm (15-CH), 111.0 ppm (10,20-CH), and 116.0 ppm (5-CH), while the internal methylenes appeared at 37.7 ppm. A proton NMR spectrum was also obtained for the anion $[15\text{-H}]^-$ in DBU/ CDCl_3 , and the *meso*-protons were observed between 9.2 and 10.2 ppm, confirming the retention of aromatic character by this species.

In order to further assess this new porphyrin analogue system, unsubstituted dibenzodicarbaporphyrins **18** and **19**, together with related tautomers, were examined by carrying out DFT calculations²⁰ at the B3LYP/6-311++G(d,p) level (Tables 1 and 2, respectively). Although X-ray structures of **5** and **15** are not available, it is worth noting that the B3LYP-optimized geometries have been reported to give good agreement with porphyrinoid structural data.²¹ For the free-base versions in these series, tautomers **18a** and **19a** were shown to be the most stable (Tables 1 and 2). Interestingly, *opp*-dicarbaporphyrin tautomer **18a** was shown to be 4.07 kcal/mol more stable than the lowest-energy *adj*-dicarbaporphyrin tautomer **19a**, even though the related tetraethylporphyrinoid **5** was reported to be somewhat unstable.⁶ Both **18a** and **19a** have four internal hydrogen atoms, leading to a somewhat crowded interior that causes significant loss of overall planarity. In **18a**, the indene rings are rotated relative to the mean macrocyclic plane by 14.59°, while the pyrrole rings are pivoted by 8.08° (Table S1 in the Supporting Information). The adjacent isomer **19a** is still more distorted. The indene rings are predicted to be rotated out of the mean macrocyclic plane by 12.02°, while the pyrrole rings are canted by 15.07° and 15.09°. Five tautomers of the *opp*-dicarbaporphyrin system were considered (Table 1). Tautomer **18b** with an internal CH_2 was shown to be 8.41 kcal/mol higher in energy, while **18c** has two internal methylene units and is 24.75 kcal/mol higher in energy. The ring distortions in **18b** are much reduced, and in **18c** the system is nearly planar (Table S1), although the 18- π -electron delocalization pathways are less favorable as they must pass through the fused benzene rings. Tautomers **18d** and **18e** are

Table 1. Calculated Energies (in hartrees), Relative Energies (in kcal/mol), and NICS Values (in ppm) for Tautomers of *opp*-Dicarbaporphyrin **18**

	18a	18b	18c	18d	18e
	-1265.0306584	-1265.0172527	-1264.9912128	-1265.0023882	-1264.9995001
	0.00	8.41	24.75	17.74	19.55
NICS(0):	-13.19	-8.53	-11.85	-1.22	-0.56
NICS(a):	+4.68	-9.42	-13.59	+3.69	+1.51
NICS(b):	-14.12	-13.61	+0.26	-1.85	-1.55
NICS(c):	-5.14	+5.26	-9.80	+3.41	+3.41
		NICS(d): -2.04		NICS(d): -9.90	NICS(d): -10.58
		NICS(e): -9.74		NICS(e): -6.11	NICS(e): -6.92
		NICS(f): -5.41		NICS(f): -6.43	NICS(f): -6.37

Table 2. Calculated Energies (in hartrees), Relative Energies (in kcal/mol), and NICS Values (in ppm) for Tautomers of *adj*-Dicarbaporphyrin 19

			
19a	19b	19c	19d
-1265.0241661	-1265.0217443	-1265.0208949	-1264.9791111
4.07	5.59	6.13	32.35
NICS(0): -11.84	NICS(0): -7.88	NICS(0): -8.04	NICS(0): -10.89
NICS(a): +5.53	NICS(a): -8.57	NICS(a): -9.28	NICS(a): -12.74
NICS(c): -14.21	NICS(b): +5.29	NICS(b): +7.73	NICS(c): -0.41
NICS(e): -4.99	NICS(c): -12.35	NICS(c): -3.69	NICS(e): -9.77
	NICS(d): -2.90	NICS(d): -12.75	
	NICS(e): -9.67	NICS(e): -9.86	
	NICS(f): -5.08	NICS(f): -4.37	
			
19e	19f	19g	19h
-1265.0067888	-1265.0079134	-1265.0047547	-1265.0023924
14.98	14.27	16.25	17.74
NICS(0): -0.25	NICS(0): -0.09	NICS(0): +1.78	NICS(0): -1.24
NICS(a): +3.27	NICS(a): +3.07	NICS(a): +3.70	NICS(a): +1.37
NICS(b): +4.21	NICS(b): +4.43	NICS(b): +1.89	NICS(b): +2.95
NICS(c): -2.43	NICS(c): -2.31	NICS(c): -8.71	NICS(c): -3.02
NICS(d): -9.34	NICS(d): -8.78	NICS(d): -3.22	NICS(d): -10.89
NICS(e): -6.29	NICS(e): -6.40	NICS(e): -6.39	NICS(e): -6.82
NICS(f): -6.16	NICS(f): -6.08	NICS(f): -6.66	NICS(f): -6.45

nonaromatic and were predicted to be 17.74 and 19.55 kcal/mol higher in energy, respectively, than tautomer **18a**. Both of these structures show a substantial divergence from planarity (Table S1). The relative energies for the series of eight *adj*-dicarbaporphyrins **19a–h** (Table 2) were calculated in comparison with the most stable *opp*-isomer **18a**. Although **19a** is the most stable tautomer, in agreement with the experimental results, tautomers **19b** and **19c** are only 1.52 and 2.06 kcal/mol higher in energy. For *adj*-dicarbaporphyrins without fused benzene rings, tautomers with internal methylene groups (e.g., **14b**) were calculated to be nearly 5 kcal/mol more stable than tautomer **14a**,¹⁸ but in this case the presence of the benzo units offsets these results to avoid having an [18]-annulene pathway that passes through a benzene ring.²² Previous DFT calculations for benzocarporphyrin had also demonstrated that inner CH₂ tautomers with 18- π -electron delocalization pathways passing through the benzo unit are significantly higher in energy than tautomers that avoid this delocalization route.²² Nevertheless, the very small differences in energy between these tautomers indicate that species like **19b** and **19c** are very accessible. As expected, the fully conjugated structure **19d** with two internal CH₂ units is much higher in energy (32.35 kcal/mol relative to **18a**), in part because of lone pair–lone pair repulsion. Tautomers **19e–h** all have interrupted conjugation due to the presence of a methylene bridge, and they have calculated energies of 14.27–17.74 kcal/mol relative to **18a**. Hence, these nonaromatic species are substantially more stable than the fully aromatic tautomer **19d** but less favored than **19a–c**. The macrocycles in both **19c** and **19d** are predicted to be flat, while

19a, **19b**, and **19e–h** all diverge considerably from planarity (Table S1).

Nucleus-independent chemical shift (NICS)²³ calculations were performed for all 13 structures (Tables 1 and 2). The NICS value at the center of **18a** [NICS(0)] was -13.19 ppm, a result that is consistent with a strongly aromatic structure, while **19a** gave a slightly smaller NICS(0) value of -11.84 ppm. As the proton NMR spectra for both **5** and **15** showed chemical shifts that were consistent with the presence of a strong diamagnetic ring current, these calculated values are broadly consistent with the experimental work. Theoretical studies indicate that the proton NMR chemical shifts observed for porphyrinoid systems are due to a combination of ring currents from the individual rings and the macrocycle as a whole.^{24–35} In **18a**, the center of ring *a* gave a NICS value of +4.68 ppm, and this appears to be caused by deshielding due to its proximity to the 18- π -electron delocalization pathway and the six- π -electron arene unit. Ring *e* gave a NICS value of -5.14 ppm, which is somewhat low for a benzene ring, while the pyrrole rings gave a value of -14.12 ppm. The latter result is due to a combination of the [18]annulene pathway and the ring current for the individual pyrrole ring. Similar results were noted for **19a**. For aromatic tautomers **18b**, **19b**, and **19c** with a single interior methylene group, the NICS(0) values were reduced to between -7.88 and -8.41 ppm (Tables 1 and 2). In **19b**, indene ring *a* with an inner CH₂ gave a NICS value of -8.57 ppm, while that for indene ring *b* was calculated as +5.29 ppm. These results make sense because the center of ring *a* lies within the 18- π -electron delocalization pathway, while ring *b* is next to but external to both this pathway and the benzene moiety and is therefore deshielded. Pyrrole ring *c* gave a strongly shielded

chloroform, the reaction mixture was washed with water and purified by column chromatography on silica, eluting with dichloromethane. A yellow-brown fraction was collected that appeared to correspond to a palladium complex of **15**. The product was poorly soluble, but a proton NMR spectrum of this derivative was obtained in CDCl₃. This showed the presence of the ethyl and methyl substituents, the benzo units, and the four *meso*-protons. However, the diatropicity of the ring system appeared to be much reduced, as the *meso*-protons appeared at 7.23 ppm (1H), 7.81 ppm (1H) and 8.03 ppm (2H). The ring system still retained a plane of symmetry, and no protons could be identified within the macrocyclic cavity. However, the precise identity of this complex was difficult to ascertain. Insertion of Pd(II) into the macrocycle may involve the loss of four protons and could give the dianionic species **20a** (Scheme 6). This species would clearly not elute from a silica column with dichloromethane, and indeed, the product was less polar than the starting material. It was possible that two protons had been retained in the structure that could not be identified in the proton NMR spectrum. However, the electrospray ionization mass spectrometry (ESI-MS) gave a cluster of peaks centered on *m/z* 1297. When the presence of multiple palladium isotopes and the fact that ESI-MS generally gives the [M + H] peak were taken into account, high-resolution MS gave a molecular formula of C₇₂H₅₆N₄Pd₃ for the complex. The carbon-13 NMR spectrum of the derivative was also obtained, but this gave no additional insights apart from confirming the presence of a plane of symmetry in the porphyrinoid ring. The mass suggested that two units of **20a** combined with three palladium ions, and the identity of the complex was finally demonstrated to be **21** by X-ray diffraction analysis (Figure 6). The structure contains two palladium-containing porphyrinoid units with a third palladium ion sandwiched between them.

This unusual complex is best described as a palladium(IV) metallocene formed by η^5 coordination of each of two (benzodicarbaporphyrinato)palladium(II) macrocycles to the third palladium atom. Compound **21** is unique both in terms of its coordination about palladium and the novel porphyrinoid

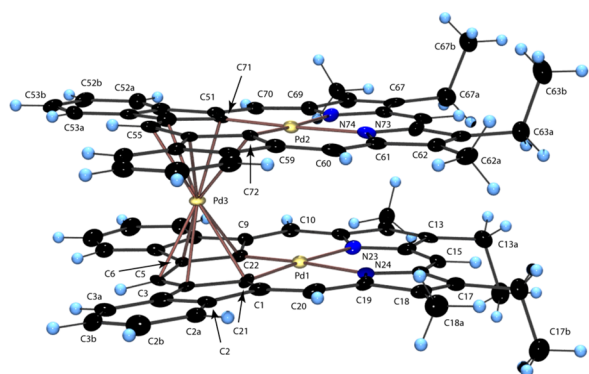


Figure 6. Color POV-Ray-rendered ORTEP III drawing (50% probability level, hydrogen atoms drawn arbitrarily small) of compound **21**. Selected bond lengths (Å): Pd3–C21 2.443(8), Pd3–C4 2.238(8), Pd3–C5 2.237(8), Pd3–C6 2.261(8), Pd3–C22 2.515(8), Pd3–C71 2.420(7), Pd3–C54 2.256(8), Pd3–C55 2.223(9), Pd3–C56 2.271(8), Pd3–C72 2.515(8). Selected bond angles (deg): C22–Pd1–N23 91.5(3), C21–Pd1–N23 176.9(3), C22–Pd1–N24 176.7(3), C21–Pd1–N24 91.5(3), N23–Pd1–N24 88.8(3), C72–Pd2–C71 88.4(3), C72–Pd2–N74 177.6(3), C71–Pd2–N74 91.0(3), C72–Pd2–N73 91.3(3), C71–Pd2–N73 178.0(3), N74–Pd2–N73 89.2(3).

coordination mode that it adopts (*vide infra*). The coordination geometry and planarity of the individual porphyrin macrocycles are similar to those observed for other palladium(II) complexes of carbaporphyrinoid systems.^{16,37,38} Each four-coordinate Pd(II) metal center adopts a typical square-planar geometry, and the porphyrinoid framework is also coplanar with this unit. In **21**, the 1.977(8) Å Pd–C21, 1.975(8) Å Pd–C22, 1.992(8) Å Pd–C71, and 1.991(8) Å Pd–C72 distances are significantly shorter than the 2.068(7) Å Pd–N23, 2.074(7) Å Pd–N24, 2.081(7) Å Pd–N73, and 2.074(7) Å Pd–N74 distances, which is consistent with the greater basicity of the carbanion ligand. Turning to the third palladium atom, a previously unknown metal-to-porphyrinoid interaction is observed in which the putative dianionic species **20b** forms a sandwich complex with the palladium(IV) ion. Metallocene complexes with the pyrrole units of porphyrins, although rare, have been described,^{39,40} and metallocenes derived from porphyrins with fused cyclopentadienyl rings have also been described.⁴¹ However, the coordination sites in **21** are unique, as they involve two different subunits and a *meso*-carbon atom. Metallocene-style bonding of carbon atoms C21, C4, C5, C6, and C22 contributes six π electrons and effectively occupies three coordination sites around the tetravalent palladium. Similarly, C71, C54, C55, C56, and C72 contribute six π electrons and occupy three more coordination sites. The average Pd–C distance of 2.338 Å between these carbon atoms and Pd3 indicates a strong bonding interaction between the ligands and the metal. With a neutral complex formed from coordination of two dianionic ligands of **20b** and an additional palladium ion, the palladium is necessarily palladium(IV) with an additional six valence electrons available for bonding. Thus, the palladium(IV) ion resides in a six-coordinate saturated 18-valence-electron bonding environment. This explains the remarkable air stability of this palladium(IV) complex. The carbon–carbon bond lengths within the macrocycles show significant variations that are consistent with reduced aromatic character, in agreement with the upfield shifts observed in the proton NMR spectrum of **21**.

Of the over 17 800 palladium-containing crystal structures in the Cambridge Structural Database (CSD, version 5.35, Feb 2014 update), less than 75 are categorized as containing palladium(IV).⁴² Only 22 of these contain Pd–C bonds, and the only crystal structure of a π -bound organometallic palladium(IV) complex is that of (allylbis(dimethylsilylpropyl)silane)(η^5 -pentamethylcyclopentadienyl)palladium(IV).⁴³ At an average of 2.39 Å, this compound exhibits slightly longer Pd–C distances than the average distance of 2.338 Å observed in **21**, supporting the statement that the metallocene bonding is strong in **21**. Fewer than 70 known structures contain η^5 -cyclopentadienyl-coordinated palladium for any Pd oxidation state. The CSD also contains seven examples of η^5 -coordinated Pd–fullerene complexes and four examples of η^6 -coordinated Pd–arene complexes. There are no examples of palladium complexes of higher hapticity, and significantly, an example of a non-cyclopentadienyl ligand that is η^5 -coordinated to palladium is unprecedented. Perhaps not surprisingly, we have managed to identify only one crystal structure of a bis(η^5 -coordinated) Pd complex, namely, bis(μ - η^5 - η^5 -1,4-bis[tris(propan-2-yl)silyl]pentalendiyl)dipalladium.⁴⁴ Complex **21** is equally unusual in terms of the nature of the porphyrinoid ligand coordination. There are over 4500 metal- and porphyrinoid-containing crystal structures, yet less than 40 include organometallic interactions with a framework *meso*-porphyrinoid carbon atom. Of these, 31

involve a direct M–C σ bond to a *meso* carbon atom. About 150 structures include organometallic interactions with the framework carbon atom α to a *meso*-carbon atom. Only two structures containing a transition metal bound to both a *meso*-carbon and the adjacent framework carbon atom have been reported. Both contain η^2 -bound ruthenium.⁴⁵ As best as we can ascertain, complex **21** is the first reported example of a porphyrinoid ligand with a *meso*-carbon-bound metal involved in greater than η^2 bonding. This is particularly significant in that it suggests that the differences observed in the organometallic chemistry of carbaporphyrins relative to their unperturbed porphyrin counterparts is likely to extend well beyond the formation of simple coordination complexes.

CONCLUSIONS

An *adj*-dibenzodicarbaporphyrin was prepared using a base-catalyzed MacDonald condensation from bis(3-indenyl)-methane and a dipyrromethane dialdehyde. DFT calculations indicated that the presence of four internal hydrogens in this structure causes significant distortions of the porphyrinoid macrocycle; however, the proton NMR spectrum was consistent with a strongly diatropic species, and this was confirmed by the nucleus-independent chemical shift values. Addition of TFA to the dicarbaporphyrin gave a monoprotated cation with an internal CH₂, and under more strongly acidic conditions a dicationic species with six internal hydrogens could be identified. Addition of DBU to solutions of the dicarbaporphyrin gave rise to an unstable anionic species, and proton NMR spectroscopy confirmed that both the protonated and deprotonated species retained highly diatropic characteristics. Reaction of the dicarbaporphyrin with palladium(II) acetate afforded a stable tripalladium complex consisting of two palladium(II) porphyrinoids encapsulating a palladium(IV) cation in a unique sandwich complex. The unusual reactivity of the *adj*-dicarbaporphyrin system indicates that many additional discoveries will be made in this area.

EXPERIMENTAL SECTION

Melting points are uncorrected. NMR spectra were recorded using a 500 MHz NMR spectrometer. ¹H NMR values are reported as chemical shifts δ (relative integral, multiplicity, coupling constant in Hz, assignment). Multiplicities are denoted as follows: s, singlet; d, doublet; t, triplet; q, quartet; m, multiplet; br, broad peak. Chemical shifts are reported in parts per million relative to CDCl₃ (¹H residual CHCl₃, 7.26 ppm; ¹³C CDCl₃ triplet, 77.23 ppm); for samples run in HCl/TFA, a small sealed tube containing C₆D₁₂ was inserted and used as a standard (¹H residual C₆HD₁₁, 1.38 ppm; ¹³C C₆D₁₂ quintet, 26.43 ppm). Coupling constants (*J*) were taken directly from the spectra. NMR assignments were made with the aid of ¹H–¹H COSY, HSQC, DEPT-135, and NOE difference proton NMR spectroscopy. Two-dimensional NMR experiments were performed using standard software. High-resolution mass spectrometry (HRMS) was carried out using a double-focusing magnetic sector instrument. ¹H and ¹³C NMR spectra for new compounds are reported in the Supporting Information.

13,17-Diethyl-12,18-dimethyldibenzo[*b,g*]-21,22-dicarbaporphyrin (15). In a 250 mL round-bottom flask, bis(3-indenyl)-methane⁴⁶ (302 mg, 1.23 mmol) was dissolved in 1% KOH in absolute ethanol (150 mL). After the solution was purged with nitrogen for 5 min, dipyrromethane dialdehyde **16**⁴⁷ (358 mg, 1.25 mmol) was added, and the resulting solution was refluxed for 4 days under a nitrogen atmosphere. The solution turned from red-brown to dark green over this period of time. The solution was diluted with dichloromethane and washed with brine (150 mL) and water (150 mL). The resulting brown organic layers were combined and dried

over sodium sulfate. The solvent was evaporated under reduced pressure to yield a dark-brown residue. The crude product was purified by column chromatography on a grade-3 alumina column, eluting with dichloromethane, followed by a silica column, again eluting with dichloromethane. The fractions were assessed by UV–vis spectroscopy. The red-brown product fractions were evaporated under reduced pressure, and the residue was recrystallized from chloroform/hexanes to give the dicarbaporphyrin (128 mg, 0.26 mmol, 21%) as a dark-blue powder.

Data for **15**: Mp: >300 °C. UV–vis (CHCl₃) λ_{max} /nm (log ϵ /M⁻¹ cm⁻¹): 324 (4.44), 368 (4.40), 396 (4.41), 455 (4.88), 479 (sh, 4.53), 542 (4.13), 579 (3.98), 658 (3.76); UV–vis (5% TFA/CHCl₃): λ_{max} (log ϵ) 327 (4.49), 418 (4.61), 451 (sh, 4.53), 670 (4.33), 734 (3.87); UV–vis (TFA/HCl): λ_{max} (log ϵ) 359 (4.59), 410 (4.47), 452 (4.72), 478 (5.07), 681 (3.79), 713 (3.89), 780 (4.17); UV–vis (10% DBU/CHCl₃): λ_{max} (log ϵ) 385 (4.35), 465 (4.99), 477 (4.93), 578 (4.06), 620 (4.12). ¹H NMR (500 MHz, CDCl₃): δ –6.24 (2H, s, 21,22-H), –5.74 (2H, s, 2 × NH), 1.70 (6H, t, *J* = 7.8 Hz, 2 × CH₂CH₃), 3.24 (6H, s, 12,18-CH₃), 3.72 (4H, q, *J* = 7.7 Hz, 13,17-CH₂), 7.44–7.50 (4H, m, 2²,3²,7²,8²-H), 8.21 (2H, d, *J* = 6.9 Hz, 2¹,8¹-H), 8.29 (2H, d, *J* = 6.9 Hz, 3¹,7¹-H), 8.91 (1H, s, 15-H), 9.09 (2H, s, 10,20-H), 9.48 (1H, s, 5-H). ¹³C NMR (CDCl₃): δ 11.4 (12,18-CH₃), 16.9 (2 × CH₂CH₃), 19.6 (13,17-CH₂), 87.1 (15-CH), 98.7 (10,20-CH), 109.2 (5-CH), 115.9 (21,22-CH), 120.0 (2¹,8¹-CH), 120.3 (3¹,7¹-CH), 125.6, 125.8, 130.4, 131.8, 133.6, 135.5, 136.0, 136.4, 140.6, 140.8. HRMS (EI): calcd for C₃₆H₃₂N₂ 492.2565, found 492.2529.

Data for monocation **15H**⁺: ¹H NMR (500 MHz, TFA/CDCl₃): δ –3.61 (2H, s, 21-CH₂), –2.04 (1H, s, 22-H), –0.40 (1H, s, NH), –0.02 (1H, s, NH), 1.62–1.67 (6H, two overlapping triplets), 3.21 (3H, s), 3.28 (3H, s), 3.73–3.80 (4H, two overlapping quartets), 7.51 (1H, t, *J* = 6.9 Hz), 7.57 (1H, t, *J* = 6.8 Hz), 8.18 (1H, d, *J* = 6.7 Hz), 8.25 (1H, d, *J* = 6.9 Hz), 8.37–8.43 (2H, m), 9.27 (1H, s), 9.36 (1H, d, *J* = 7.4 Hz), 9.46 (1H, d, *J* = 7.5 Hz), 9.54 (1H, s), 9.76 (1H, s), 9.92 (1H, s). ¹³C NMR (TFA/CDCl₃): δ 10.98, 11.02, 16.6, 16.7, 19.8, 37.2, 105.4, 107.2, 121.0, 121.8, 122.9, 123.5, 127.9, 129.5, 130.5, 131.8, 133.1, 133.4, 138.7, 142.1, 142.3, 142.9, 143.2, 144.0, 145.1, 146.5, 146.6, 147.6.

Data for dication **15H₂²⁺**: ¹H NMR (500 MHz, HCl/TFA): δ –4.09 (4H, s, 21,22-CH₂), –0.49 (2H, s, 2 × NH), 1.74 (6H, t, *J* = 7.4 Hz, 2 × CH₂CH₃), 3.52 (6H, s, 12,18-CH₃), 4.00 (4H, q, *J* = 7.4 Hz, 13,17-CH₂), 8.87 (2H, t, *J* = 6.8 Hz, 3²,7²-H), 8.98 (2H, t, *J* = 6.9 Hz, 2²,8²-H), 10.07 (2H, d, *J* = 7.5 Hz, 2¹,8¹-H), 10.25 (2H, d, *J* = 7.3 Hz, 3¹,7¹-H), 10.49 (1H, s, 15-H), 11.06 (2H, s, 10,20-H), 12.08 (1H, s, 5-H). ¹³C NMR (HCl/TFA): δ 10.3 (12,18-CH₃), 15.8 (2 × CH₂CH₃), 20.1 (13,17-CH₂), 38.8 (21,22-CH₂), 111.0 (15-CH), 112.0 (10,20-CH), 117.0 (5-CH), 125.0 (2¹,8¹-CH), 126.8 (3¹,7¹-CH), 133.9 (3²,7²-CH), 137.90 (2²,8²-CH), 137.96, 138.1, 145.2, 146.1, 147.9, 150.5, 150.7, 166.7.

Bis(μ_2 - η^2 -13,17-Diethyl-12,18-dimethyldibenzo[*b,g*]-21,22-dicarbaporphyrinato)dipalladium(II)palladium(IV) (21). Palladium (II) acetate (15 mg, 0.067 mmol) was added to a solution of dibenzocarbaporphyrin **15** (15 mg, 0.030 mmol) in acetonitrile (20 mL), and the resulting mixture was refluxed under an atmosphere of nitrogen for 40 min. The solution turned from pale yellow to dark brown over this period of time. The resulting solution was diluted with chloroform and washed with water. The organic layers were dried over sodium sulfate, and the solvent was evaporated under reduced pressure. The residue was purified by column chromatography on silica, eluting with dichloromethane, and the first fraction (yellow-brown) contained the product. The solvent was evaporated under reduced pressure, and the residue was recrystallized from chloroform/hexanes to give the palladium complex (13 mg, 0.010 mmol, 66%) as a brown powder. Mp: >300 °C. UV–vis (CHCl₃): λ_{max} (log ϵ) 285 (4.64), 322 (sh, 4.55), 384 (4.53), 434 (4.51), 570 (sh, 4.03). ¹H NMR (500 MHz, CDCl₃, 310 K): δ 1.37 (12H, t, *J* = 7.6 Hz), 2.58 (12H, s), 2.93–3.07 (8H, m), 6.84 (4H, t, *J* = 7.2 Hz), 7.225 (4H, t, *J* = 7.3 Hz), 7.234 (2H, s), 7.32 (4H, d, *J* = 7.3 Hz), 7.48 (4H, d, *J* = 7.3 Hz), 7.81 (2H, s), 8.03 (4H, s). ¹³C NMR (CDCl₃, 310 K): δ 10.6, 17.3, 19.1, 87.4, 106.1, 112.5, 113.3, 118.3, 120.1, 126.3, 129.1, 129.9,

131.3, 136.4, 139.2, 142.2, 144.6, 147.1, 148.3. HRMS (ESI): calcd for $C_{72}H_{57}N_4^{105}Pd_3$, 1292.1736, found 1292.1731.

Computational Studies. Geometry optimization calculations were performed using Gaussian 09, revision D.01,⁴⁸ running on a Linux-based PC. Energy-minimization calculations of the porphyrinoid systems were performed using DFT with the B3LYP functional and the 6-311++G(d,p) basis set. Mercury 3.1 running on an OS X platform, as provided by the CCDC (www.ccdc.cam.ac.uk/mercury/), was used to visualize the optimized structures. The resulting Cartesian coordinates of the molecules can be found in the Supporting Information. NICS calculations were also performed using Gaussian 09, revision D.01,⁴⁸ running on a Linux-based PC. NICS values were computed by the GIAO method⁴⁹ using DFT at the B3LYP/6-31+G(d,p) level at several positions in each molecule. NICS(0) was calculated at the mean position of all of the non-hydrogen atoms. NICS(a), NICS(b), NICS(c), NICS(d), NICS(e), and NICS(f) values were obtained by applying the same method to the mean positions of the non-hydrogen atoms constituting the individual rings of each macrocycle.

■ ASSOCIATED CONTENT

■ Supporting Information

Cartesian coordinates and HOMO and LUMO surfaces for all of the calculated tautomers; experimental details for the crystallographic study; and selected ¹H NMR, ¹H–¹H COSY, HMQC, ¹³C NMR, DEPT-135, MS, and UV–vis spectra. This material is available free of charge via the Internet at <http://pubs.acs.org>.

■ AUTHOR INFORMATION

Corresponding Author

tdlash@ilstu.edu

Notes

The authors declare no competing financial interest.

■ ACKNOWLEDGMENTS

This work was supported by the National Science Foundation (Grant CHE-1212691) and the Petroleum Research Fund, administered by the American Chemical Society. The authors also thank the National Science Foundation (Grant CHE-1039689) for providing funding for the X-ray diffractometer.

■ REFERENCES

- (1) (a) Lash, T. D. In *The Porphyrin Handbook*; Kadish, K. M., Smith, K. M., Guilard, R., Eds.; Academic Press: San Diego, CA, 2000; Vol. 2, pp 125–199. (b) Lash, T. D. *Synlett* **2000**, 279–295. (c) Lash, T. D. *Eur. J. Org. Chem.* **2007**, 5461–5481.
- (2) Lash, T. D. In *Handbook of Porphyrin Science—With Applications to Chemistry, Physics, Material Science, Engineering, Biology and Medicine*; Kadish, K. M., Smith, K. M., Guilard, R., Eds.; World Scientific: Singapore, 2012; Vol. 16, pp 1–329.
- (3) Pawlicki, M.; Latos-Grazynski, L. In *Handbook of Porphyrin Science—With Applications to Chemistry, Physics, Material Science, Engineering, Biology and Medicine*; Kadish, K. M., Smith, K. M., Guilard, R., Eds.; World Scientific: Singapore, 2010; Vol. 2, pp 104–192.
- (4) Lash, T. D.; Hayes, M. J. *Angew. Chem., Int. Ed. Engl.* **1997**, *36*, 840–842.
- (5) (a) Lash, T. D.; Hayes, M. J.; Spence, J. D.; Muckey, M. A.; Ferrence, G. M.; Szczepura, L. F. *J. Org. Chem.* **2002**, *67*, 4860–4874. (b) Liu, D.; Lash, T. D. *J. Org. Chem.* **2003**, *68*, 1755–1761.
- (6) Lash, T. D.; Romanic, J. L.; Hayes, M. J.; Spence, J. D. *Chem. Commun.* **1999**, 819–820.
- (7) (a) Muckey, M. A.; Szczepura, L. F.; Ferrence, G. M.; Lash, T. D. *Inorg. Chem.* **2002**, *41*, 4840–4842. (b) Lash, T. D.; Colby, D. A.; Szczepura, L. F. *Inorg. Chem.* **2004**, *43*, 5258–5267.
- (8) Lash, T. D. *Org. Lett.* **2011**, *13*, 4632–4635.

- (9) (a) Liu, D.; Lash, T. D. *Chem. Commun.* **2002**, 2426–2427. (b) Liu, D.; Ferrence, G. M.; Lash, T. D. *J. Org. Chem.* **2004**, *69*, 6079–6093. (c) Jain, P.; Ferrence, G. M.; Lash, T. D. *J. Org. Chem.* **2010**, *75*, 6563–6573.
- (10) (a) Hayes, M. J.; Spence, J. D.; Lash, T. D. *Chem. Commun.* **1998**, 2409–2410. (b) Lash, T. D.; Muckey, M. A.; Hayes, M. J.; Liu, D.; Spence, J. D.; Ferrence, G. M. *J. Org. Chem.* **2003**, *68*, 8558–8570.
- (11) (a) Morgenthaler, J. B.; Peters, S. J.; Cedeño, D. L.; Constantino, M. H.; Edwards, K. A.; Kamowski, E. M.; Passini, J. C.; Butkus, B. E.; Young, A. M.; Lash, T. D.; Jones, M. A. *Bioorg. Med. Chem.* **2008**, *16*, 7033–7038. (b) Taylor, V. M.; Cedeño, D. L.; Muñoz, D. L.; Jones, M. A.; Lash, T. D.; Young, A. M.; Constantino, M. H.; Esposito, N.; Vélez, I. D.; Robledo, S. M. *Antimicrob. Agents Chemother.* **2011**, *55*, 4755–4764.
- (12) For examples of doubly N-confused porphyrins, see: (a) Furuta, H.; Maeda, H.; Osuka, A. *J. Am. Chem. Soc.* **2000**, *122*, 803–807. (b) Maeda, H.; Osuka, A.; Furuta, H. *J. Am. Chem. Soc.* **2003**, *125*, 15690–15691.
- (13) Graham, S. R.; Colby, D. A.; Lash, T. D. *Angew. Chem., Int. Ed.* **2002**, *41*, 1371–1374.
- (14) Xu, L.; Lash, T. D. *Tetrahedron Lett.* **2006**, *47*, 8863–8866.
- (15) (a) Lash, T. D.; Colby, D. A.; Idate, A. S.; Davis, R. N. *J. Am. Chem. Soc.* **2007**, *129*, 13801–13802. (b) Lash, T. D.; Lammer, A. D.; Idate, A. S.; Colby, D. A.; White, K. *J. Org. Chem.* **2012**, *77*, 2368–2381.
- (16) Zhang, Z.; Ferrence, G. M.; Lash, T. D. *Org. Lett.* **2009**, *11*, 101–104.
- (17) Lash, T. D.; Lammer, A. D.; Ferrence, G. M. *Angew. Chem., Int. Ed.* **2012**, *51*, 10871–10875.
- (18) AbuSalim, D. I.; Lash, T. D. *J. Org. Chem.* **2013**, *78*, 11535–11548.
- (19) Lash, T. D. *Chem.—Eur. J.* **1996**, *2*, 1197–1200.
- (20) (a) Ghosh, A. *Acc. Chem. Res.* **1998**, *31*, 189–198. (b) Ghosh, A. In *The Porphyrin Handbook*; Kadish, K. M., Smith, K. M., Guilard, R., Eds.; Academic Press: San Diego, CA, 2000; Vol. 7, pp 1–38.
- (21) Alonso, M.; Geerling, P.; De Proft, F. *Chem.—Eur. J.* **2013**, *19*, 1617–1628.
- (22) AbuSalim, D. I.; Lash, T. D. *Org. Biomol. Chem.* **2013**, *11*, 8306–8323.
- (23) Schleyer, P. v. R.; Maerker, C.; Dransfeld, A.; Jiao, H.; Hommes, N. J. R. v. E. *J. Am. Chem. Soc.* **1996**, *118*, 6317–6318.
- (24) Juselius, J.; Sundholm, D. *J. Org. Chem.* **2000**, *65*, 5233–5237.
- (25) Steiner, E.; Fowler, P. W. *Org. Biomol. Chem.* **2003**, *1*, 1785–1789.
- (26) Steiner, E.; Fowler, P. W. *Org. Biomol. Chem.* **2004**, *2*, 34–37.
- (27) Steiner, E.; Soncini, A.; Fowler, P. W. *Org. Biomol. Chem.* **2005**, *3*, 4053–4059.
- (28) Steiner, E.; Fowler, P. W. *Org. Biomol. Chem.* **2006**, *4*, 2473–2476.
- (29) Aihara, J.-i. *J. Phys. Chem. A* **2008**, *112*, 5305–5311.
- (30) Aihara, J.-i.; Kimura, E.; Krygowski, T. M. *Bull. Chem. Soc. Jpn.* **2008**, *81*, 826–835.
- (31) Aihara, J.-i.; Makino, M. *Org. Biomol. Chem.* **2010**, *8*, 261–266.
- (32) Otero, N.; Fias, S.; Radenkovic, S.; Bultinck, P.; Graña, A. M.; Mandado, M. *Chem.—Eur. J.* **2011**, *17*, 3274–3286.
- (33) Nakagami, Y.; Sekine, R.; Aihara, J.-i. *Org. Biomol. Chem.* **2012**, *10*, 5219–5229.
- (34) Aihara, J.-i.; Nakagami, Y.; Sekine, R.; Makino, M. *J. Phys. Chem. A* **2012**, *116*, 11718–11730.
- (35) Wu, J. I.; Fernández, I.; Schleyer, P. v. R. *J. Am. Chem. Soc.* **2013**, *135*, 315–321.
- (36) Lash, T. D. *Chem.—Asian J.* **2014**, *9*, 682–705.
- (37) Lash, T. D.; Colby, D. A.; Graham, S. R.; Ferrence, G. M.; Szczepura, L. F. *Inorg. Chem.* **2003**, *42*, 7326–7338.
- (38) Lash, T. D.; Young, A. M.; Von Ruden, A. L.; Ferrence, G. M. *Chem. Commun.* **2008**, 6309–6311.
- (39) (a) Dailey, K. K.; Yap, G. P. A.; Rheingold, A. L.; Rauchfuss, T. B. *Angew. Chem., Int. Ed. Engl.* **1996**, *35*, 1833–1835. (b) Cuesta, L.; Karnas, E.; Lynch, V. M.; Sessler, J. L.; Kajonkiya, W.; Zhu, W.; Zhang,

M.; Ou, Z.; Kadish, K. M.; Ohkubo, K.; Fukuzumi, S. *Chem.—Eur. J.* **2008**, *14*, 10206–10210. (c) Cuesta, L.; Karnas, E.; Lynch, V. M.; Chen, P.; Shen, J.; Kadish, K. M.; Ohkubo, K.; Fukuzumi, S.; Sessler, J. L. *J. Am. Chem. Soc.* **2009**, *131*, 13538–13547.

(40) Senge, M. O. *Angew. Chem., Int. Ed. Engl.* **1996**, *35*, 1923–1925.

(41) (a) Wang, H. J. H.; Jaquinod, L.; Nurco, D. J.; Vicente, M. G. H.; Smith, K. M. *Chem. Commun.* **2001**, 2647–2648. (b) Wang, H. J. H.; Jaquinod, L.; Olmstead, M. M.; Vicente, M. G. H.; Kadish, K. M.; Ou, Z.; Smith, K. M. *Inorg. Chem.* **2007**, *46*, 2898–2913.

(42) Allen, F. H. *Acta Crystallogr.* **2002**, *B58*, 380–388.

(43) Suginome, M.; Kato, Y.; Takeda, N.; Oike, H.; Ito, Y. *Organometallics* **1998**, *17*, 495–497.

(44) Summerscales, O. T.; Rivers, C. J.; Taylor, M. J.; Hitchcock, P. B.; Green, J. C.; Cloke, F. G. N. *Organometallics* **2012**, *31*, 8613–8617.

(45) Yamaguchi, S.; Shinokubo, H.; Osuka, A. *J. Am. Chem. Soc.* **2010**, *132*, 9992–9993.

(46) Li, H.; Stern, C. L.; Marks, T. J. *Macromolecules* **2005**, *38*, 9015–9027.

(47) Lash, T. D. *Tetrahedron* **1998**, *54*, 359–374.

(48) Frisch, M. J.; Trucks, G. W.; Schlegel, H. B.; Scuseria, G. E.; Robb, M. A.; Cheeseman, J. R.; Scalmani, G.; Barone, V.; Mennucci, B.; Petersson, G. A.; Nakatsuji, H.; Caricato, M.; Li, X.; Hratchian, H. P.; Izmaylov, A. F.; Bloino, J.; Zheng, G.; Sonnenberg, J. L.; Hada, M.; Ehara, M.; Toyota, K.; Fukuda, R.; Hasegawa, J.; Ishida, M.; Nakajima, T.; Honda, Y.; Kitao, O.; Nakai, H.; Vreven, T.; Montgomery, J. A., Jr.; Peralta, J. E.; Ogliaro, F.; Bearpark, M.; Heyd, J. J.; Brothers, E.; Kudin, K. N.; Staroverov, V. N.; Kobayashi, R.; Normand, J.; Raghavachari, K.; Rendell, A.; Burant, J. C.; Iyengar, S. S.; Tomasi, J.; Cossi, M.; Rega, N.; Millam, N. J.; Klene, M.; Knox, J. E.; Cross, J. B.; Bakken, V.; Adamo, C.; Jaramillo, J.; Gomperts, R.; Stratmann, R. E.; Yazyev, O.; Austin, A. J.; Cammi, R.; Pomelli, C.; Ochterski, J. W.; Martin, R. L.; Morokuma, K.; Zakrzewski, V. G.; Voth, G. A.; Salvador, P.; Dannenberg, J. J.; Dapprich, S.; Daniels, A. D.; Farkas, Ö.; Foresman, J. B.; Ortiz, J. V.; Cioslowski, J.; Fox, D. J. *Gaussian 09*, revision D.01; Gaussian, Inc.: Wallingford, CT, 2009.

(49) Wolinski, K.; Hinton, J. F.; Pulay, P. *J. Am. Chem. Soc.* **1990**, *112*, 8251–8260.